IOP Conf. Series: Journal of Physics: Conf. Series **1115** (2018) 032045 doi:10.1088/1742-6596/1115/3/032045

Introduction of hydrogen into titanium by plasma methods

N N Nikitenkov, E D Daulethanov, Yu I Tyurin, Le Zhang, D O Sivin, V S Sypchenko and M S Syrtanov

National Research Tomsk Polytechnic University, 30 Lenin Ave., Tomsk, 634050, Russia

E-mail: nikitenkov@tpu.ru

Abstract. The introduction of hydrogen into titanium VT1-0 by the methods of plasma-immersion ion implantation (PIII) from the hydrogen plasma of a source with a heated cathode and into high-frequency discharge (HFD) plasma was studied. Modes of installations for introduction are chosen proceeding from the requirement of the maximum content of hydrogen in the samples. It is established that saturation from the HFD-plasma leads to a significant enrichment to a depth of 1.2 μm, at the introduction of hydrogen by the PIII this depth is 0.6 μm. The hydrogen content of 0.06 wt.% in the samples after saturation in the HFD plasma, and 0.049 wt.% after PIII. During PIIII (with an energy of 0.9-1.5 keV), hydrogen is strongly scattered by the surface of the sample and is captured predominantly by surface defects (including those created by the ions themselves), as well as by vacancies in the near-surface layers. Upon saturation from the HFD-plasma, hydrogen diffuses into the interior of the sample and settles in interstices and at grain boundaries. At the same time, saturation from the HFD plasma and PIII lead to significant change in the crystal parameters and the creation of hydride phases.

1. Introduction

Titanium and its alloys are widely used as structural materials in various industries [1-4]. The penetration and accumulation of hydrogen in titanium products lead to a change in their physic-chemical and operational properties and, ultimately, hydrogen embrittlement and destruction [5]. The shape and intensity of such changes depend on the state of hydrogen in the material [6]. Hydrogen in titanium can be in the form of hydrides or in a dissolved state [7, 8]. Determination of the amount, distribution and state of accumulated hydrogen under various treatment methods is necessary for the development of methods for preventing hydrogen embrittlement.

In the literature, there are many works [9-16] devoted to the study of hydrogen accumulation and storage in titanium alloys during hydrogenation from the gas (hydrogen) condition and from electrolytes. At the same time, there are few papers devoted to the introduction of hydrogen into titanium from plasma. In the present work, hydrogen introduced from the hydrogen plasma of a high-frequency discharge [17] and from gas discharge plasma based on a plasma source with a heated cathode [18] in the device [19].

Thus, the aim of this work was to study the mechanisms of hydrogen storage in titanium by irradiating high-intensity pulsed-periodic beams of low-energy hydrogen ions from a gas-discharge plasma and saturation from high-frequency discharge hydrogen plasma.

2. Materials and methods of research

For the study, samples of titanium VT1-0 with sizes 20×20×1 mm were prepared. The surface of titanium samples prior to irradiation with hydrogen were mechanically polished in order to remove surface oxide films.

Hydrogen concentrations measured with a hydrogen analyzer RHEN602 of LECO corporation. The hydrogen distribution profiles obtained with a glow-charge plasma spectrometer of the Horiba GD-Profiler 2. The phase composition and structural parameters of the samples studied on a XRD-7000S diffractometer using the X-ray radiation line CuKα. The obtained spectra of X-ray diffraction processed with using the software POWDER CELL 2.4.

The thermo-stimulated spectra of gas egress (TSGE) from the samples obtained at a vacuum assembly for the study of thermo- and radiation-stimulated gas outlet [20]. The linear heating rate was 1 degree per second. The activation energy (E_a) of the H_2 yield was calculated in accordance with [21]

Hydrogen accumulation in titanium during irradiation with powerful pulses of hydrogen plasma carried out at the installation with the apparatus scheme, which presented in [19]. The method based on extraction of ions from the free plasma boundary, their acceleration in a high-voltage charge-separation layer and the formation of a beam with a high current density by ballistic focusing of ions.

Saturation from HFD-plasma carried out at the apparatus described in [17]; the sample is not earthed and is not bias, that is, it is "suspended".

Table 1 shows the most effective parameters for the introduction of hydrogen by the PIII method (in bold italics) and saturation from the HFD plasma. The most effective saturation mode from the HFD-plasma selected in preliminary experiments earlier (shown in the last line).
The designations of iPIII from table 1 will be used in the text below.

Table 1. Modes of introduction of hydrogen by the method of PIII and from HFD-plasma.

Modes PIII							
Sample	Irradiation time, min	Current density in the pulse, A/cm^2	Pulse frequency, imp/s	Bias on the sample, V	Pulse duration, μs	Temperature, °C	Dose, ion/ cm^2
Ti_{PIII0}	60	0.3	10^5	1200	4	800	$2.7\cdot10^{21}$
Ti_{1PIII}	***60***	***0.11***	***10^5***	***900***	***3***	***360***	***$7.4\cdot10^{20}$***
Ti_{2PIII}	60	0.17	10^5	900	3	390	$1.1\cdot10^{21}$
Ti_{P3III}	20	0.11	10^5	900	3	380	$2.5\cdot10^{20}$
Ti_{4PIII}	50	0.17	10^5	900	3	390	$9.6\cdot10^{20}$
From the HFD plasma							
Sample		Saturation time, min.		Temperature, °C		Pressure, Torr	
Ti_{HFD}		95		400		10^{-1}	

3. Results and discussion

3.1. Concentration of hydrogen after PIII and HFD-plasma

The results of measuring the hydrogen concentration are shown in table 2. It can be seen from the table that the hydrogen concentration in the samples after saturation in the HFD plasma is greater than after the PIII.

These differences are apparently because the accelerated hydrogen ions are strongly scatters on surface of sample. If sample immersed in the HFD plasma, the ions and hydrogen atoms are easily captured by surface defects and diffuse into the sample volume under action of concentration gradient and temperature.

Table 2. Results of hydrogen concentration in the titanium alloy VT1-0.

Sample Ti	Concentration, ppm
$Ti_{initial}$	74.7
Ti_{1PIII}	502.5
Ti_{2PIII}	236.9
Ti_{HFD}	603.2

3.2. X-ray studies

The results of the X-ray analysis of the samples after PIII and HFD plasma shown in table 3 and in figure 1.

Table 3. Results of XRDA after PIII and HFD plasma.

Sample	Detected phases	Content of phases, vol.%	Lattice parameters, Å
Original	Ti_hexagonal	100	a = 2.941; c = 4.668
Ti_{PIII1}	Ti_hexagonal	100	a=2.9526; c=4.6843
Ti_{PIII2}	Ti_hexagonal	100	a=2.9515; c=4.6840
Ti_{HFD}	Ti_hexagonal	100	a=2.9510; c=4.6841

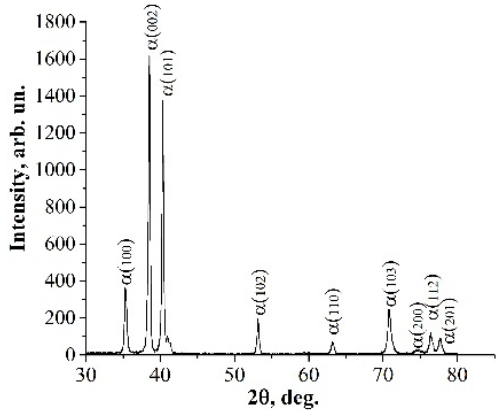

a)

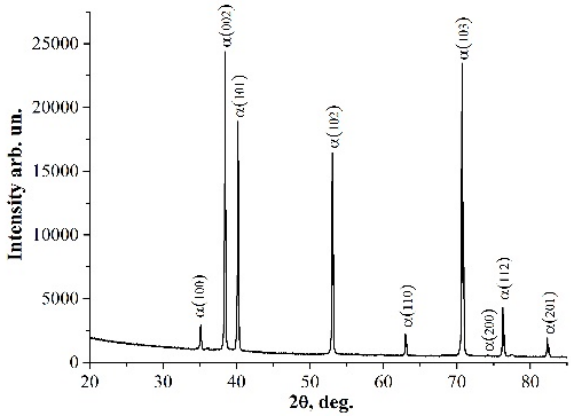

b)

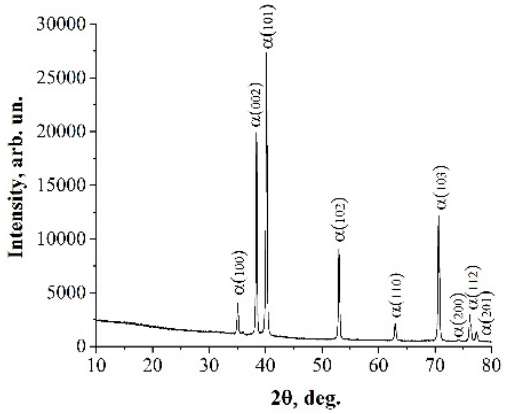

c)

Figure 1. X-ray diffraction patterns of titanium samples: a) initial, b) after 1PIII; c) after HFD plasma.

As can be seen from the table 3, the detected phases, the volume content of the phases and the lattice parameters are the same for all samples. At the same time, the lattice parameters with embedded hydrogen are noticeably larger than for the original sample. This indicates the penetration of hydrogen into the lattice of grain crystallites. Figure 1 shows that all α -Ti phases are observed on all titanium samples, and narrow and high diffraction peaks are due to the fact that the material is well crystallized.

3.3. The layer-by- layer the elements distribution

Figure 2 shows the distribution profiles of the elements in the samples of the titanium alloy VT1-0 before and after PIII and saturation from the HFD plasma (see designations of modes in table 1). It can be seen that on the initial sample, the high hydrogen content is at the depths of 0.05-0.25 μm with a decrease to 0.4 μm (figure 2a). On a Ti_{PIII} sample, a high hydrogen content is found at depths of 0.05-0.25 μm with a decay greater than 0.6 μm (figure 2b). And on a sample of Ti_{PIII2}, the concentration of high contents is at depths of 0.05-0.3 μm with a decay greater than 0.8 μm (figure 2c).

Thus, saturation from the HFD plasma leads to a significant enrichment to a depth of 1.2 μm, with the introduction of hydrogen by the PIII method, this depth is 0.6 μm.

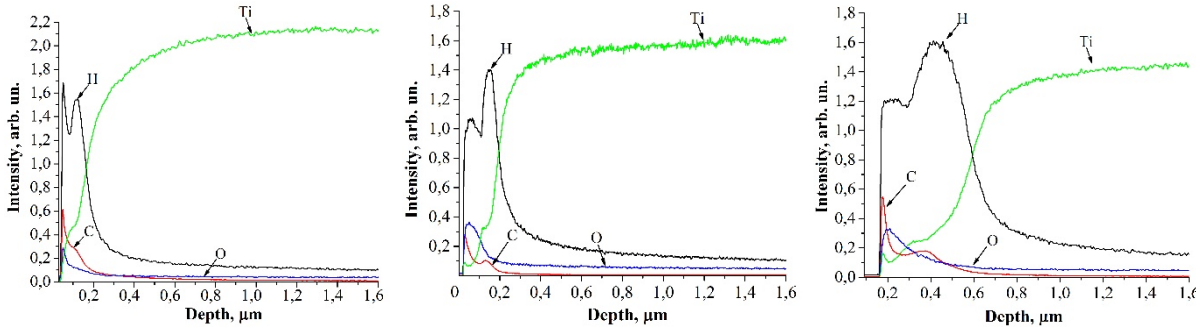

Figure 2. The layer-by-layer distribution of the elements after 1PIII and HFD plasma: a) the initial; b) after 1PIII, c) after HFD plasma.

3.4. Temperature spectra of gas evolution from samples after PIII and HFD plasma

Figure 3 shows the TSGE spectra of hydrogen H_2 and other hydrogen-containing molecules from samples of the titanium alloy VT1-0 after 1PIII and after saturation in the HFD plasma; and in table 4 the results of integrating these spectra are compared with the measured hydrogen concentrations in the samples. It can be seen that the composition of gases, leaving the samples, is the same, but their quantitative content varies greatly. In particular, the high yield of OH at saturation from the HFD plasma compared with PIII. The opposite, with respect to OH, the ratio is observed for the NH molecule. This fact explain by the enrichment the working atmosphere by the release of oxygen at action HFD generator from the quartz tube, which is the hull of the plasma reactor. Table 4 shows that, as was noted above from the sample of Ti_{HFD} after the HFD plasma, the integral values of the yield H (respectively, the concentration of hydrogen) and hydrogen-containing molecules (CH, NH, OH) are larger in comparison with PIII. In addition, the carbon of Ti_{1PIII} sample is the largest in comparison with other samples. In addition to the Ti_{PIII} sample, the integral values of the yield of hydrogen (H) and hydrogen-containing NH, OH molecules are higher. Thus, it can be said that the yields intensity of the hydrogen, carbon and the hydrogen-containing molecules differ significantly, this is obviously due to the gas medium in which saturating samples. That is, the composition of media, and especially if these media are in different aggregate states, can strongly influence the process of hydrogen absorption by a solid; the figure below confirms this.

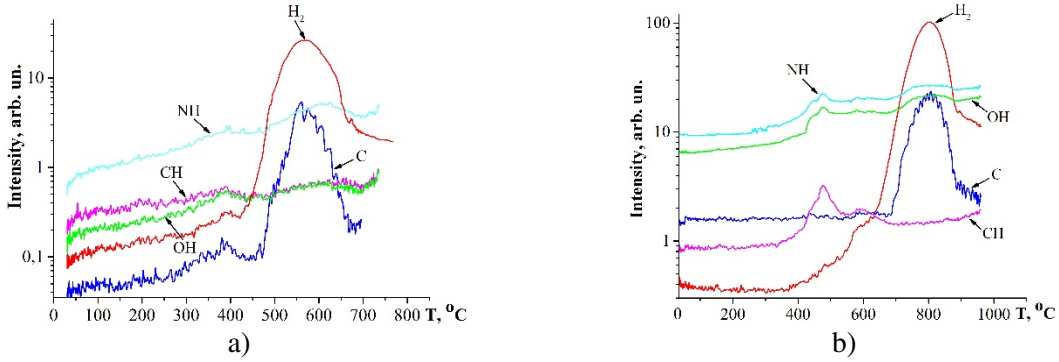

Figure 3. Spectra of hydrogen, carbon, and other hydrogen containing molecules from samples: a) after PIII1, b) after HFD-plasma.

Table 4. The results of integration of the TSGE curves, the relative yield Ii/I_H (where I_i are the output of carbon and hydrogen-containing molecules; I_H is the integral output of H_2 in comparison with the hydrogen concentration (C_H) in the samples (in ppm) obtained with RHEN602.

Sample	The value of the integral (arb. un.) and relative to H (rel. un.) outputs				
$Ti_{Initial}$	H	C	CH	NH	OH
	571	96	28	170	295
I_i/I_H	-	0.17	0.049	0.297	0.626
C_H	74.7 ppm				
Ti_{1PIII}	H	C	CH	NH	OH
	3932	390	110	455	627
I_i/I_H	-	0.1	0.059	0.247	0.368
C_H	502.5 ppm				
Ti_{HFD}	H	C	CH	NH	OH
	4234	122	172	559	687
I_i/I_H	-	0.03	0.072	0.233	0.262
C_H	603.2 ppm				

Figure 4 compares the TSGE H_2 offsets from the samples of the penetrated hydrogen implantation using the PIII methods and from the HFD plasma. The arrows in the curves show the temperature at the maxima of the spectra, and corresponding to them, the desorption activation energy. In the temperature spectrum of hydrogen from the PIII sample (figure 4, curve 1) two peaks are observed, one low intense, corresponding to a temperature of 400°C and one higher intense at a temperature peak of 564° C. That corresponds to activation energy of desorption 1.9 eV and 2.4 eV.

This indicates that in these samples, at least 2 types of hydrogen traps are formed during irradiation. On the curve 2, the peak corresponds to a temperature of 803°C, with a desorption activation energy of 3.1 eV.

Here, apparently, hydrogen is captured on volumetric interstices. The difference between the behavior of curve 1 and 2 is explained, apparently, by the mechanism of hydrogen penetration, which consists in the following. When irradiated with low-energy hydrogen ions, most of the ions dissipate on the surface and do not pass into the volume. The HFD plasma "surrounds" the sample surface at thermal energies, and hydrogen is captured by surface defects with subsequent diffusion to volume defects.

Significant differences in the TSGE spectra are explained by the formation of various types of traps with significantly different parameters of irradiation and saturation from the plasma of the HFD. It is assumed that at 400-567 °C – hydrogen is trapped on surface defects.

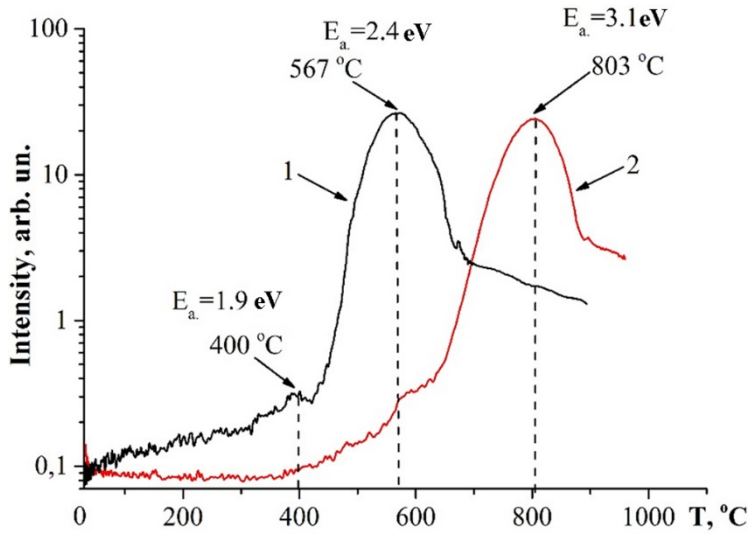

Figure 4. TSGE H_2 spectra from samples of the titanium alloy VT1-0 saturated with the methods: 1) Ti_{1PIII}, 2) from the HFD-plasma.

4. Conclusion

Saturation from the HFD plasma of the titanium alloy VT1-0 leads to a significant enrichment to a depth of 1.2 μm; at the hydrogen introduction by the PIII this depth is 0.6 μm. The hydrogen concentration in the samples after saturation in the HFD plasma is larger (by 17%) compared to the hydrogen concentration after PIII with the saturation and penetration regimes selected for the maximum hydrogen content.

Saturation from the high-frequency plasma and PIII irradiation leads to noticeable change in the crystalline parameters and does not lead to the creation of hydride phase. Consequently, hydrogen in the samples is in a dissolved state and this state deforms the lattice of crystallites. This indicates that the hydrogen is in the interstices, as the proton dimensions are very small.

These regularities explained by strong backscattering of the accelerated hydrogen ions by the surface, and by the formation of surface defects that are "traps" of hydrogen, so that little penetration of hydrogen into the sample occurs. At the same time, when the sample is "suspended" in the HFD plasma, the ions and the hydrogen atoms are easily captured by the surface defects, diffuse into the sample volume and settle in interstitial sites and on the grain boundaries.

References

[1] Gurrappa I 2005 *Mater. Characterization* **51** 131
[2] Schutz R, Watkins H B 1998 *Mater. Sci. Engineer. A* **243** 305
[3] Yamada M 1996 *Mater. Sci. Engineer. A* **213** 8
[4] Brewer W D, Bird R K and Wallace T A 1998 *Mater. Sci. Engineering A* **243** 299
[5] Madina V, Azkarate I 2009 *Intern. J. Hydrog. Energy* **34** 5976
[6] Lunarska E, Chernyayeva O, Lisovytskiy D, et al. 2010 *Mater. Sci. Engineer:C* **30** 181
[7] Furuya Y, Takasaki A and Mizuno K 2007 *J. Alloys and Compounds* **446–447** 447
[8] Eliezer D, Tal-Gutelmacher E, Cross C E, et al. 2006 *Mater. Sci. Engineer. A*. **421** 200
[9] Kudiyarov V N, Leader A M, Pushilina N S, Timchenko N A 2014 *Technical Physics* **59** 1378
[10] Perevalova O B, Panin A V, Kretova O M and Teresov A D 2014 *Bulletin of the Russian Academy of Sciences: Physics* **78** 706
[11] Kudiyarov V N and Leader A M 2013 *Fundamental research* **10** 3466
[12] Hruska P, Cızek J, Knapp J, Lukac F, Melikhova O, Maskova S, Havela L and Drahokoupil J 2017 *International journal of Hydrogen Energy* **42** 22557
[13] Pokhmurskii V I, Vynar V A, Vasyliv Ch B and Ratska N B 2013 *Wear.* **306** 47
[14] Burnyshev I N and Kalyuzhny D G 2014 *Chemical physics and mesoscopy* **16** 250

[15] Burnyshev I N, Kalyuzhny D G, Lys V F and Tarasov V V 2015 *Chemical physics and mesoscopy* **17** 565
[16] Cherdantsev Yu P, Chernov I P and Tyurin Yu I 2008 *Methods for studying metal-hydrogen systems: textbook* (Tomsk: TPU Publishing House) 286 p
[17] Sypchenko V S 2016 The interaction of hydrogen with a thin film Al_2O_3 on nanocrystalline titanium. Thesis for the degree of cand. Phys.-math sciences Tomsk 122 p
[18] Koval N N and Schanin P M. http://ipms.bscnet.ru/conferenc/krnd_sem/doc-2/Kovalj.pdf
[19] Ryabchikov A I, Sivin D O 2012 *Russian Physics Bulletin* **12** 76
[20] Nikitenkov N N, Khashkhash A M, Shulepov I A, Khoruzhii V D, Tyurin Y I, Chernov, I P and Kudryavtseva E N 2011 *Russian Journal of Non-Ferrous Metals* **52** 115
[21] Woodruff D P, Delchar T A 1986 *Modern techniques of surface science* (Cambridge: University Press)